The Mass Transfer Mechanism of Columns Packed With sub-3µm Shell Particles and its Reproducibility for Low- and High-Molecular Weight Compounds

by Fabrice Gritti
Department of Chemistry, University of Tennessee, Knoxville, TN 37996-1600, USA

The mass transfer mechanism and the column-to-column reproducibility of the efficiency of 2.1 and 4.6mm x 100mm columns packed with the same batch of 2.7µm Poroshell120-C_{18} core-shell particles was investigated. The accurate measurement of the band broadening phenomena provided unambiguous explanations for their exceptional kinetic performance. With respect to columns packed with fully porous particles, the gain of efficiency observed for small molecules was due to a 40% and 30% reduction of the trans-column eddy dispersion and longitudinal diffusion HETP terms, respectively. For larger molecules, it was explained by the 40% reduction of the solid-liquid mass transfer resistance HETP term. The 25% smaller efficiency of the 2.1 versus the 4.6mm I.D. columns stemmed from the increasing contribution of the trans-column eddy dispersion (wall effects) to the overall eddy dispersion with decreasing the column I.D. Relative standard deviations of 8% were found for the distribution of the optimum HETPs of these 2.1 mm and 4.6mm I.D. columns, respectively.

The concept of shell, core-shell, or superficially porous particles is not new. Some fifty years ago, the terminology of pellicular stationary phases was employed by Cs. Horvath when he and his co-workers prepared some new ion-exchange columns designed for the HPLC separations of high-molecular weight compounds of biological interest [1]. They suggested the idea of coating 50µm glass beads (impermeable cores) with a thin layer of anion-active resin. On the same line, Knox recommended the use of thin films of liquid stationary phase in liquid-liquid chromatography [2] and Parish proposed preparing a shallow surface layer of ion-exchange groups around cross-linked polystyrene beads for the separation of metal ions [3]. The incentive for the preparation of such new stationary phase architectures was clear: decrease the solid-liquid mass transfer resistances by decreasing the average diffusion distance of the analytes across the stationary phase volume. Back then, the average particle sizes were as large as 50 to 100µm, e.g., so that the column efficiencies were essentially dictated by the mass transfer resistance between the particle volume and the mobile phase. Reducing the porous layer thickness led then to a significant improvement in the resolution of complex mixtures [4-6].

However, over the next forty years, the competition of packing materials made with high-purity, fine fully porous particles increased ceaselessly over time [7]. Additionally, pellicular particles have a much lower loading capacity than that of fully porous particles so the injected sample concentrations should be kept to a minimum in order to avoid column overloading and nefarious peak distortion. So, pellicular particles encountered little commercial success (50µm Corasil I and II, Zipax, Pellicosil [8, 9], and 5µm Poroshell [10]) and fell into oblivion until, in 2007, they were resuscitated as the modern sub-3 µm Halo shell particles [11] (Advanced Material Technologies, Inc). Most remarkably, these sub-3µm shell particles provided column efficiencies comparable to those achieved with sub-2µm fully porous particles [12] with the advantage of operating at about twice lower back pressure [13]. So, it became possible to achieve ultra-high column performance using the standard 400 bar instruments, provided that some low cost modifications (smaller I.D. connectors, smaller detection cell volume) be made to these instrument [14,15].

Rapidly, new brands of sub-3µm superficially porous particles emerged on the market with the 2.7µm Ascentis Express (Supelco, Inc), 2.6µm Kinetex (Phenomenex, Inc), 2.7µm Poroshell120 (Agilent Technologies, Inc), 2.6µm Accucore (Thermo Scientific, Inc), 2.7µm Nucleoshell (Macherey-Nagel, Inc), and 2.6µm Sunshell (Chromanik, Inc). The names of shell, core-shell, or superficially porous particles replaced the old terminology "pellicular particles" because of the large thickness of the porous layer relatively to the particle diameter. All these particles were made of a 1.6 to 1.9µm solid silica cores, covered with a 0.35 to 0.50µm thick porous shell. Such particle architecture solved the issue of the low loading capacity since 60 to 75% of their volume versus only less than 15% for the old pellicular particles is now accessible to the analytes [16].

As a result of their increasing success, five main questions/debates surged about the exceptional kinetic performance of columns packed with shell particles: (1) Which mass transfer mechanism can properly justify why columns packed with shell particles provide lower reduced plate heights than those packed with conventional fully porous particles? Based on widespread chromatographic beliefs, most of the literature reports and all the advertising brochures suggested hastily that this was due to the reduction of the diffusion path across the stationary phase and to the narrow size distribution of this new packing material [11, 49]. This has never been proven experimentally and theoretically, especially for small molecules. (2) What is the column-to-column reproducibility of such high-performance columns? No data are yet available in the literature on this topic. They are critical for both the manufacturers, who want to minimise their rebuttal levels, and for

the analysts, who seek for robust separation processes. (3) What is the most suitable core-shell architecture for the separation of large molecular weight compounds? The tradeoff between peak resolution (thin shell) and column loading (thick shell) should be investigated [15, 17]. (4) What is the impact of the column inner diameter on the kinetic performance of these columns? The careful study of the column wall effects on the homogeneity of the packed bed needs to be investigated [18]. (5) What is the lifetime stability of these columns? This is of paramount importance for those who buy these columns and want to minimise their expenses over a long term period.

The above issue (5) is out of the scope of this work because it would require a very long investigation time. In this work, answers to questions (1), (2), (3), and (4) will be provided based on the rigorous measurement of the individual mass transfer resistance terms in the van Deemter equation (longitudinal diffusion, solid-liquid mass transfer resistance, and eddy dispersion terms) for two series of six 2.1mm x 100mm and six 4.6mm x 100mm columns packed with the same batch of 2.7µm Poroshell120-C_{18} shell particles (Agilent Technologies, Little Fall, DE, USA). The relative impact of each HETP term on the overall column performance and their column-to-column reproducibility are then discussed for both low- and high-molecular weight compounds.

Theory

In this section, the basic equations that provide the different reduced HETP contributions (longitudinal diffusion, solid-liquid mass transfer resistance, and eddy dispersion) to the total reduced HETP in columns packed with shell particles were listed. The reader is referred to references [19-23] for the derivation and the experimental validation of these equations in the case of columns packed with sub-3µm shell particles. Note that the reference linear velocity used in these equations is the interstitial linear velocity, *u*. The specific reduced velocity, ν, is given by

$$\nu = \frac{u d_p}{D_m} = \frac{F_v d_p}{\varepsilon_e \pi R_c^2 D_m}$$

(1)

where d_p is the average particle size, F_V is the flow rate, ε_e is the external porosity of the column, R_c is the column inner radius, and D_m is the bulk molecular diffusion coefficient of the analyte. Note that the d_p values used in this work are those provided by the column manufacturer (commercial particle diameter).

1. Longitudinal diffusion term (B/ν)

The reduced longitudinal diffusion HETP term, h_{Long}, accounts for the natural relaxation of the axial concentration along the chromatographic zone. It is best written as [21, 23]:

$$h_{Long} = \frac{B}{\upsilon} = \frac{2\left(\gamma_e + \frac{1-\varepsilon_e}{\varepsilon_e}\frac{1-\rho^3}{1+\frac{\rho^3}{2}}\Omega\right)}{\upsilon}$$

(2)

where *B* is the longitudinal diffusion coefficient, which can be directly measured from a series of peak parking experiments [16]. In Eq. (2), γ_e is the external obstruction factor, which was found around 0.65 for 4.6 x 100mm columns packed with sub-3µm non-porous silica spheres with a narrow particle size distribution (RSD around 5%) and a bed voidage or external porosity, ε_e, close to 40% [24]. ρ is the ratio of the solid core to the particle diameter and Ω is the ratio of the sample diffusivity in the porous shell to that in the bulk phase. In RP-HPLC and for average mesopore size of the porous shell around 100 Å, Ω varies from about 0.15 (non-retained) to 1.50 (moderately retained) for small molecules [22, 25]. For larger molecule such as insulin, Ω varies from about 0.01 (non-retained) to 0.20 (moderately retained) [26].

2. Solid-liquid mass transfer resistance term (Cν)

This HETP term, $h_{Liquid\text{-}Solid}$, accounts for the band broadening due to the velocity difference between the moving eluent and the stationary phase. If we consider spherical particles and extract the parameter Ω from Eq. (1) , this term is written [22]:(4)

$$h_{Liquid-Solid} = C\upsilon = \frac{1}{15}\frac{1-\rho^3}{1+\frac{\rho^3}{2}}\left(\frac{k_1}{1+k_1}\right)^2\left[\frac{1+2\rho+3\rho^2-\rho^3-5\rho^4}{(1+\rho+\rho^2)}\right]\frac{1}{B-2\gamma_e}\upsilon$$

where k_1 is the zone retention factor (~ 3.0 for compounds with retention factors of about 2). *C* is the solid-liquid mass transfer coefficient. Typically ρ ranges between 0.60 and 0.75 for the different brands of sub-3µm core-shell particles currently available in the field. Eventually, for such ρ values, *C* is typically equal to about 0.005 and 0.050 for small and large (insulin) retained molecules, respectively.

3. Eddy dispersion term (A)

The eddy dispersion term, h_{Eddy}, accounts for all the sources of unevenness of the flow velocity distribution taking place in the interstitial mobile phase. Velocity biases in a chromatographic columns are found across different scale lengths, from the inter-particle distance $\left(\approx\frac{d_p}{10}\right)$ to a few particle diameters and to the column inner radius $\left(\frac{d_c}{2}\right)$ [19]. This HETP term may be indirectly assessed by subtraction of the previous two HETP terms from the overall reduced plate height, *h*. *h* is derived from the first (μ_1) and the second central (μ'_2) moments of the band after correction of these moments for the extra-column volume contributions ($\mu_{1,ex}$ and $\mu'_{2,ex}$) due to the band dispersion along the instrument channels [27]. So, the true value of the reduced column HETP is given by:

$$h = \frac{L}{d_p}\frac{\mu'_2 - \mu'_{2,ex}}{(\mu_1 - \mu_{1,ex})^2}$$

(5)

and the eddy diffusion term is measured as

$$h_{Eddy} = h - h_{Long} - h_{Liquid-Solid} = A(\upsilon)$$

(6)

$A(\upsilon)$ is the eddy dispersion HETP term. In contrast with what is generally held, it depends, a priori, on the linear velocity [19]. Unlike the standard United States Pharmacopeial (USP) convention, note that the determination of the column reduced plate height from the accurate moments of the elution band is the only correct method to assess the true column efficiency [27-29]. It takes the contribution of peak tailing into proper account. The classical method based to the band width at any fractional peak height is highly inaccurate.

Experimental

1. Equipments and columns

The 1290 Infinity HPLC system (Agilent Technologies, Waldbronn, Germany) instrument used in this work includes a 1290 Infinity Binary Pump with Solvent Selection Valves and a programmable auto-sampler. The injection volume is drawn into one end of the 20µL injection loop and flushed back into the eluent stream (FILO mode of transfer). The instrument is equipped with a

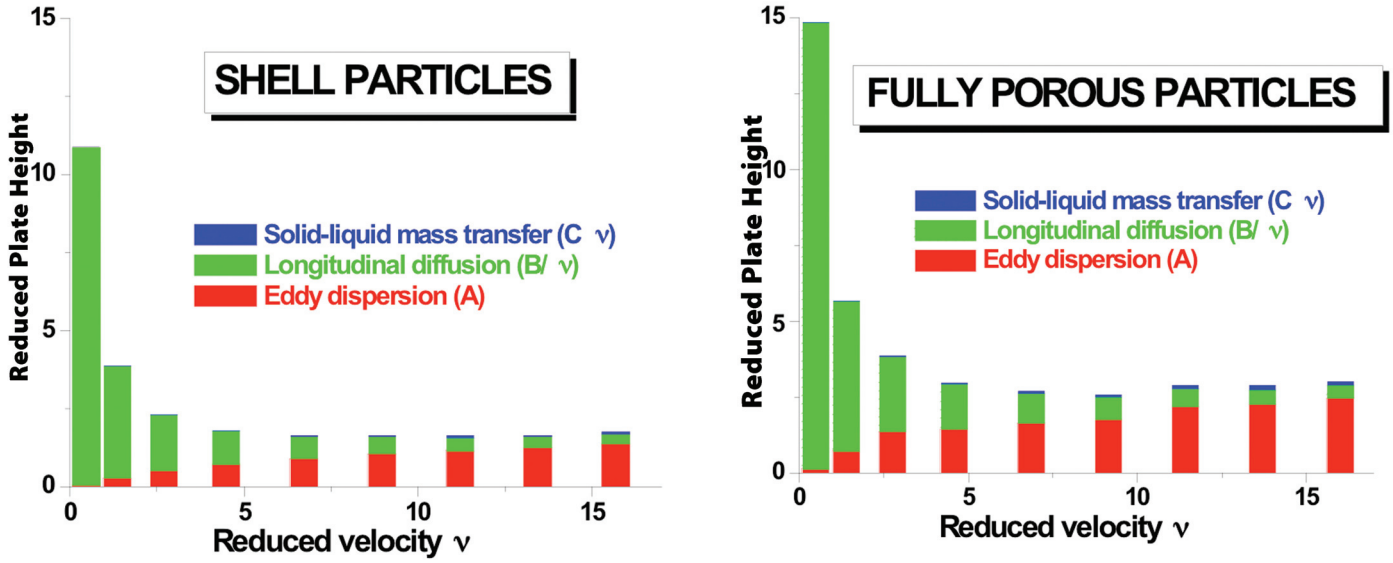

Figure 1: Contributions of the longitudinal diffusion (green), eddy dispersion (red), and solid-liquid mass transfer resistance (blue) terms to the overall reduced plate height of 4.6mm x 100mm columns packed with 2.7µm Poroshell120-C_{18} core-shell particles (Left) and 2.5µm Luna-C_{18}(2) fully porous particles (Right). Analyte: naphthalene (k~3). Mobile phase: acetonitrile/water, 65/35, v/v. T=297 K.

multi-diode array UV-VIS detection system. It is controlled by the Chemstation software. The sample trajectory in the equipment involves passage through (1) one end of the 20µL injection loop, which is attached to the injection needle, (2) a small volume (1µL) needle seat capillary (115µm I.D., 100mm long) located between the injection needle and the injection valve (the total volume of the grooves and connection ports in the valve is around 1.2µL), (3) two 130µm x 25cm long Viper capillary tubes (3.3µL each) offered by the manufacturer (Dionex, Germering, Germany) placed, one before, the second after the column, and (4) A small volume detector cell, 0.8µL, which has a 10mm optical path. The total extra-column volume is close to 9µL. The extra-column peak variances of naphthalene (k~3) account at most for 2% and 23% of the total peak variance measured for the 4.6 and 2.1mm I.D. columns, respectively.

Twelve columns (six of dimension 4.6mm x 100mm and six of dimension 2.1mm x 100mm) among a total of forty columns (twenty of dimension 4.6mm x 100mm and twenty of dimension 2.1mm x 100mm) packed with the same batch of 2.7µm Poroshell120-C_{18} core-shell particles were used. For each column I.D., the manufacturer (Agilent Technologies, Little Fall, DE, USA) performed their quality control test for all twenty columns, measured their efficiency for naphthalene by complying with the USP convention (half-height peak width method), and provided us with two columns at about the centre of the efficiency distribution and two other pairs of columns at about two standard deviations above and below the mean efficiency. Two additional 4.6mm x 100mm columns packed with fully porous 2.5µm Luna-C_{18}(2) and non-porous 3.3µm silica particles were generously offered by Phenomenex (Torrance, CA, USA).

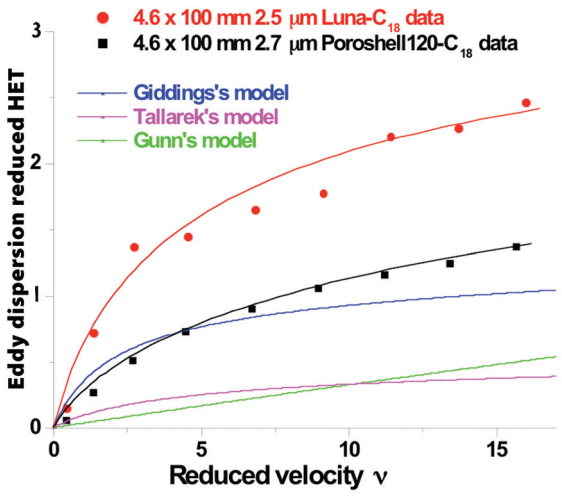

Figure 2: Comparison between the experimental reduced eddy dispersion of naphthalene (k~3) for two commercial chromatographic columns packed with fully porous (black square symbols) and shell (full red circle symbols) and some theoretical expressions assuming the infinite diameter column (blue, pink, and green solid lines).

2. ISEC, PP, and HETP measurements

The external porosity, ε_e, of each chromatographic column was measured from inverse size-exclusion chromatography (ISEC) using the linear extrapolation of the plot of the elution volumes of the four heaviest polystyrene standards versus the hydrodynamic radius to zero. The eleven polystyrene standards used (MW=590, 1100, 3680, 6400, 13200, 31600, 90000, 171000, 560900, 900000, and 1870000) were purchased from Phenomenex (Torrance, CA, USA). The peak parking (PP) method [30] was applied to measure the longitudinal coefficient B in Eq. (2) and the solid-liquid mass transfer resistance coefficient C in Eq. (3) of the small analyte, naphthalene. The flow rates were set at 0.063 and 0.300mL/min for the 2.1 and 4.6mm I.D. columns, respectively. The respective injection volumes of the diluted (< 0.1g/L) naphthalene solution were 1 and 2µL. The parking times were set at 1, 15, 30, 60, and 90 min. The PP method was also used to measure the diffusion coefficient of naphthalene in the mobile phase (H_2O/CH_3CN, 35/65, v/v) by using the column packed with non-porous particles and a reference standard analyte (thiourea) for which the diffusion coefficient is known accurately (D_m=1.33 x 10^{-5} cm^2/s in pure water and at T=25°C [31, 32]). Eventually, the diffusion coefficient of naphthalene is equal to 1.66 x 10^{-5} cm^2/s in the acetonitrile-water eluent and at 25°C. The HETP of naphthalene were recorded for the following sequence of flow rates: 0.063, 0.125, 0.208, 0.313, 0.417, 0.521, 0.625, 0.729, and 0.833mL/min (2.1mm I.D. columns) and 0.10, 0.30, 0.60, 1.0, 1.5, 2.0, 2.5, 3.0, and 3.5mL/min (4.6mm I.D. columns). The sampling rates were adjusted from 2.5 to 80 Hz in order to record at least 96 data points per peak before the numerical integration and the determination of the first and second central moments.

3. Accuracy and precision of the experimental A, B, and C coefficients

The relative accuracy and precision of the measurement of the three mass transfer resistance coefficients were recently investigated upon studying the reproducibility of the efficiency of columns packed with sub-3µm core-shell particles [33]. The measurement accuracy assesses the largest relative distance with respect to the true value. They are equal to 11%, 9%, and 21% for the A, B, and C coefficients, respectively. The precision of the experimental protocol takes into account the largest random fluctuations (lab temperature and injection-to-injection first and second central moments) that cannot be controlled during the experiments. Eventually, the relative precisions with respect to the mean value were found better than 5% (for $\nu > 3$), 4%, and 6% for the A, B, and C coefficients, respectively.

Results and Discussions

1. Mass transfer mechanism of small molecules: naphthalene.

Naphthalene has a molecular weight of 128g/mol for a molecular size of about 6 Å. It has access to most of the internal particle volume and surface area. The average ambient temperature was 296.6 K and the mobile phase a 65/35 (v/v) premixed solution of acetonitrile and water. The diffusion coefficient of naphthalene was measured at $1.66 \times 10^{-5} cm^2/s$. The plots of the reduced HETPs, *h*, of this retained compound (k ~3) versus the reduced velocity, ν, were acquired for six 4.6mm x 100mm columns packed with the same batch of 2.7µm Poroshell120-C_{18} shell particles. For the sake of comparison, the same measurements were repeated on a 4.6mm x 100mm column packed with 2.5µm fully porous Luna-C_{18}(2) particles. The Luna-C_{18}(2) particles were selected because, under the above experimental conditions, the relative diffusivity of naphthalene across these particles with respect to its bulk diffusion coefficient (Ω=1.61) is nearly identical to that across the shell of the Poroshell particles (Ω=1.59). Additionally, their average particle size is very similar to that of the Poroshell120-C_{18} particles, so, the pressure drops along the two columns were similar. Figure 1 shows the experimental contributions of the average B/ν, Cν, and A(ν) HETP terms to the overall reduced HETP for the Poroshell column (left graph) and compares them with those measured for the Luna column (right graph). Three important remarks can be made:

(1) The longitudinal diffusion coefficients (green colour), B, of the Poroshell columns are 27% smaller than that of the Luna column. This is in good agreement with Eq. (2), which predicts a relative decrease of 31% for the B coefficient of the Poroshell columns (ε_e=0.37, γ_e=0.62, ρ =0.63, Ω =1.59 → B=4.89) with respect to that of the Luna column (ε_e =0.35, γ_e =0.60, ρ =0, Ω =1.61 → B=7.11). Note that the diminution of the reduced longitudinal diffusion term caused by the presence of the non-porous cores at the optimum reduced velocity (ν~8) is of the order of 0.25 h unit. This represents a non-negligible gain in column efficiency for the analyst (~ 25 000 plate counts per meter for 2.7µm particles).

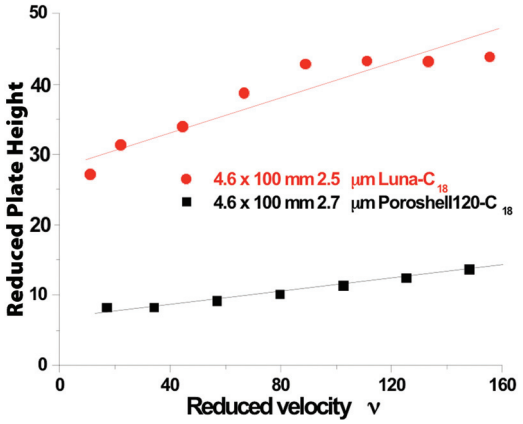

Figure 3: Plots of the total reduced plate height of insulin versus the reduced velocity measured on two commercial columns packed with fully (Luna) and superficially (Poroshell) porous particles. T=297 K. Mobile phase: acetonitrile/water/TFA, 31/69/0.1, v/v/v. Sample volume injected: 1µL. Sample concentration: < 0.05g/L.

(2) The eddy dispersion HETP term (red colour), A, of the Poroshell columns measured at the optimum velocity and above are about 40% lower than that measured for the Luna column. It decreases from about 1.7 (Luna) to only 1.0 (Poroshell) for ν=8. The reasons for this large diminution of the A term have yet to be revealed. Unlike widespread belief among the chromatographic community, it has been proven both experimentally [34-38] and theoretically [39] that the tight particle size distribution (PSD) of these core-shell particles (RSD of the PSD around 5% versus 20-30% for conventional particles) could not explain the reduction of the sample band dispersion along beds packed with them. This is even so true that the external porosity of columns packed with shell particles are larger than those of conventional columns and that axial dispersion is expected to increase with increasing the external porosity of bulk random packings [40]. To demonstrate this point, Figure 2 plots the experimental eddy dispersion HETP terms of the Poroshell and Luna columns versus the reduced velocity and compare them to those expected for bulk random packings of impermeable spheres in absence of wall effects (e.g., infinite diameter column). The theoretical models were those derived by Gunn [41], Giddings [19], and Tallarek [18]. In all models, the external porosity was assumed to be 0.36. The mobile phase velocity biases assumed in these models are limited to those taking place over short scale lengths, from the short inter-particle distances (trans-channel eddy diffusion) to a few particle diameters (short-range inter-channel eddy diffusion). Remarkably, the experimental data are systematically larger than all the predicted ones because the axial dispersion models do not take in account the band spreading caused by the presence of the wall in real confined system. The arrangement of the particles in the vicinity of the stainless steel wall is different from that in the centre bulk region of the column [18]. This explains the origin of the nefarious trans-column eddy dispersion HETP, which was found larger in 4.6mm x 100mm columns packed with fully

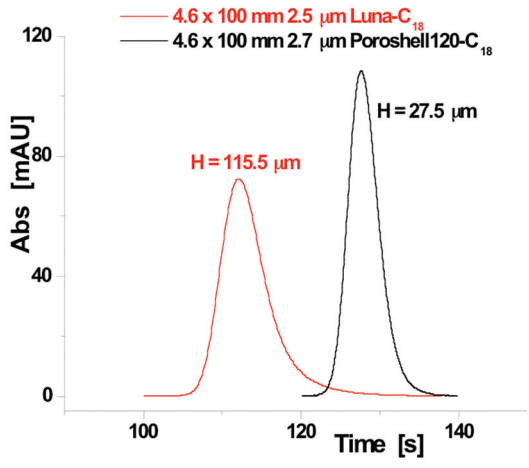

Figure 4: Examples of band profiles of insulin measured on two commercial columns packed with fully (Luna) and superficially (Poroshell) porous particles. Flow rate: 1.6mL/min. Same experimental conditions as in Figure 3.

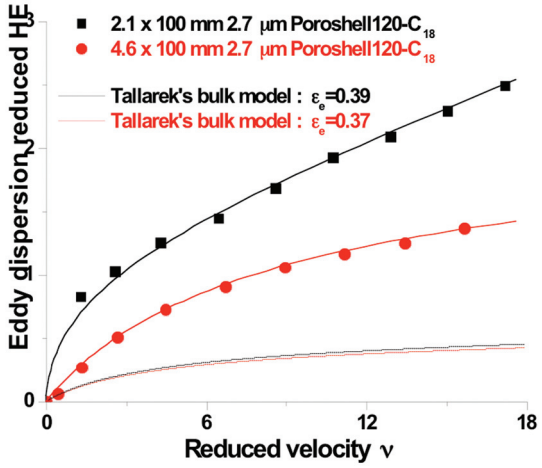

Figure 5: Comparison between the experimental reduced eddy dispersion HETP terms of naphthalene (k~3) for two commercial columns (Poroshell120) of different inner diameters packed with the same batch of superficially porous particles (full symbols) and those predicted from the mass transport simulation assuming an infinite column diameter for two different external porosities, εe (thin solid lines). Analyte: naphthalene (k~3).

porous particles than in those packed with shell particles. Possibly, the external roughness of the shell particles would help generate a more radially homogeneous bed structure than that of beds consolidated with smooth conventional fully porous particles. The particle-to-particle and particle-to-wall shear stresses would be larger for rough than for smooth particles and their strain would remain smaller during the bed consolidation. Rheological measurements using large amount of both these packing materials are yet to be carried out to confirm/refute this hypothesis.

(3) The contribution of the solid-liquid mass transfer resistance HETP term (blue colour), Cν, to the total reduced plate height was found negligible for both types of columns.

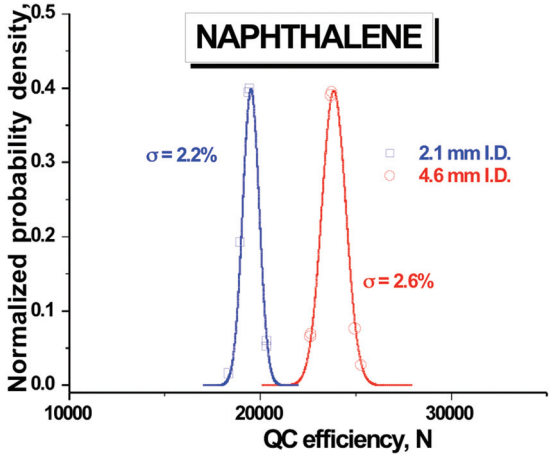

Figure 6: Efficiency distributions estimated for two sets of six 10cm long columns packed with the same batch of 2.7µm Poroshell120-C_{18} core-shell particles. Analyte: naphthalene (k~3).

Even at the highest reduced velocity, it still accounts for less than 5% of the total HETP. At optimum velocity, this term decreased from 0.08 to 0.04 h unit, a negligible gain in column efficiency. Therefore, against a widespread accepted belief around the business of core-shell particles, the advantage of these new sub-3µm particles has nothing to do with the 40% reduction of the average diffusion path across these particles. This is definitely true for small molecules for which the reduced velocity does not exceed 20. In the next section it is possible to analyse the overall mass transfer resistance of a much higher molecular weight compound, insulin.

2. Mass transfer mechanism of large molecules: insulin.

Insulin has a molecular weight of 5.8 kDa for a molecular size of about 32 Å. It is then partly excluded from the mesoporous volume and surface area of the poroshell120-C_{18} particles (120 Å average mesopore size). The average ambient temperature was 296.6 K and the mobile phase a 31/69/0.1 (v/v/v) premixed solution of acetonitrile, water, and trifluoroacetic acid. This particular mobile phase composition allows providing a retention factor of insulin around 2 at low flow rates. It increases up to about 5 at the maximum flow rate used due to the impact of pressure on the retention of insulin in RPLC. The diffusion coefficient of insulin was measured at 1.29 x 10^{-6}cm^2/s, e.g., a value one order of magnitude smaller than that measured for the small molecule naphthalene. Therefore, the range of reduced velocity accessible extends from about 10 to 160. The plots of the total reduced plate heights of insulin are shown in Figure 3. Remarkably, they are about four times larger for the Luna (h=43) than for the Poroshell (h=10) columns. Because the longitudinal diffusion HETP term, B/ν, is negligible for large molecules and the eddy dispersion HETP, A, is controlled by a flow mechanism (A tends toward values of about 2 and 3 for the Poroshell and Luna columns, respectively, as shown in Figure 2), the large h values reported in Figure 3 are attributed to the slow mass transfer of insulin across the porous particles (Cν) and to a slight thermodynamic column overloading. Figure 4 compares the peak shapes recorded on both columns at the same flow rate of 1.6mL/min. The peak of insulin skews more for the Luna (100 Å) than for the Poroshell (120 Å) columns as the result of the large exclusion of insulin from the pore volume distribution of the Luna particles. This is consistent with the smaller retention time observed although the Luna particles are fully porous. Additionally, the rate of increase of the reduced plate height with the reduced velocity is 2.7 times larger for the fully porous (C=0.115) than for the core-shell (C=0.043) particles. According to Eq. 3 and 4 (k_1~3), the relative diffusivity, Ω, of insulin with respect to its bulk diffusion (1.29 x 10^{-6} cm^2/s) are estimated at 0.09 (Luna) and 0.15 (Poroshell120). To summarise, for large molecules, the column efficiency is controlled by both the exclusion (peak skew) and the slow diffusivity (broad peak) of the compound from and across the mesoporous volume.

Unlike small molecules, the high resolution of large molecules requires the packing material to be designed with a large core-to-particle ratio, ρ, and wide mesopores (from 200 to 300 Å). Column manufacturers realised how important these structural parameters were and they recently released on the market new 3.6µm core shell particles (Aeris Widepore from Phenomenex, Inc) with a ratio ρ around 0.9 and an average pore size around 200 Å. The reduced C coefficient was found as small as 0.027 [42].

3. Impact of the column diameter on its kinetic performance: 2.1 vs. 4.6mm I.D.

Smaller I.D. columns can be used to reduce the amount of solvent consumed provided the band broadening caused by the instrument can be kept to a minimum by reducing the connecting tube and detection cell volumes [14]. However, the wall effects (or the ratio of the particle diameter to the column diameter) increase, therefore, it is crucial to quantify the possible loss of column efficiency when reducing the column I.D. Figure 5 compares the average eddy dispersion of naphthalene along its

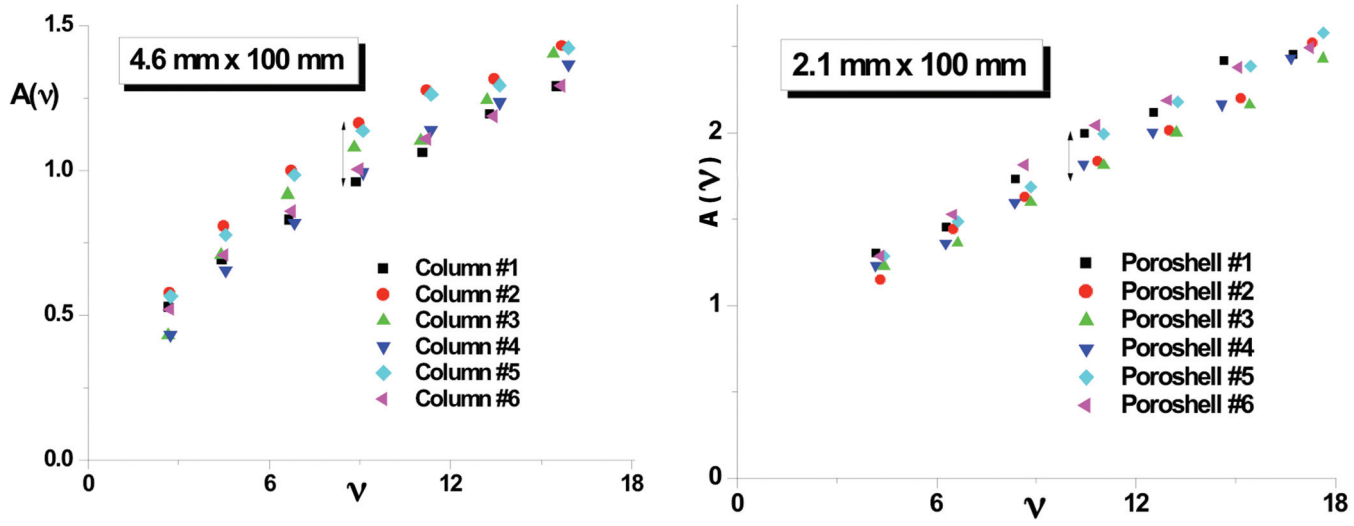

Figure 7: Column-to-column reproducibility of the reduced eddy dispersion term, A, versus the reduced velocity, ν, for 4.6mm x 100mm (Left) and 2.1mm x 100mm (Right) columns packed with the same batch of 2.7µm Poroshell120-C_{18} core-shell particles. Analyte: naphthalene (k~3).

migration through six 2.1 and 4.6mm x 100mm columns packed with the very same batch of Poroshell120-C_{18} particles. Again, recall that these HETPs were corrected for the extra-column band spreading contributions. Eventually, at constant reduced velocity, it is found that the narrow-bore columns are intrinsically less efficient (-25%) than the 4.6mm I.D. columns because of a larger axial dispersion coefficient. This is partly explained by the larger external porosities of the 2.1 mm I.D. columns (0.39 versus 0.37 for 4.6mm I.D. columns). According to Tallarek's simulations [40], this increase of the column external porosity would only lead to a 7% decrease of the column efficiency by considering the sole trans-channel and short-range inter-channel eddy dispersion terms (infinite diameter column). Therefore, the efficiency loss observed for the narrow-bore columns is necessarily due to the increase of the trans-column eddy dispersion term (+ 40%). As the column I.D. is decreasing, the impact of the radial structure heterogeneity of the packed bed on the sample band dispersion is growing and is lowering the column performance. As shown in Figure 5, today's column efficiencies are mostly dictated by the bulk-to-wall or trans-column eddy dispersion term. Better resolution will be achieved by optimising slurry packing methods which are strongly tied to the nature of the packing material [43].

4. Reproducibility of the efficiency of columns packed with 2.7µm Poroshell particles

In section 1, the advantage of packing 4.6mm I.D. columns with shell than with fully porous particles was demonstrated. The issue of column-to-column reproducibility for such high-performance chromatographic columns was then tackled. This task was already investigated by Kele et al. for a series of five 4.6mm x 250mm or 4.6mm x 150mm columns packed with the same batch of conventional 5µm fully porous particles. Four different brands of particle were tested including the Symmetry-C_{18} [44], Kromasil-C_{18} [45], Luna-C_{18}(2) [46], and Vydac 218TP-C_{18} [47] particles. By using a buffered (pH=7.0) methanol-water (65/35, v/v/) mixture as the mobile (1mL/min) phase, a HP1100 as the HPLC instrument, and by complying with the United States Pharmacopeial (USP) convention for the measurement of the column efficiency (half-height peak width method) [48], the authors found for naphthalene RSDs of 1.2 (Symmetry), 1.9 (Kromasil), 2.3 (Luna), and 2.0% (Vydac). Note that the RSDs of the retention times were 0.6, 0.5, 0.6, and 0.5%, respectively.

For the sake of comparison, the same RSDs were measured for naphthalene on two series of six 4.6mm x 100mm and six 2.1mm x 100mm columns packed with the same batch of 2.7 µm Poroshell-C_{18} particles. The mobile phases were mixtures of acetonitrile and water (60/40 and 55/45, v/v, respectively) and the flow rates were 2.0 and 0.55mL/min. The USP convention was applied by the manufacturer for the measurement of the column efficiencies, which were reported in the QC sheets sent along with the columns. Figure 6 shows the best estimated efficiency distributions and their corresponding RSDs of 2.6% (4.6mm I.D.) and 2.2% (2.1mm I.D.), which are comparable to those measured with conventional fully porous. The RSDs of the retention times were equal to 0.9 and 1.1%, respectively.

Let us recall that the USP convention is not an accurate method for the measurement of the true column efficiency because it does not treat peak tailing properly. Instead, the true column efficiencies were measured from the numerical integration of each experimental peak profile. The column-to-column reproducibility of the longitudinal diffusion (B), solid-liquid mass transfer resistance (C), and eddy dispersion (A) HETP terms were then assessed. Remarkably, for both column diameters, the reproducibility levels of the B (0.8%) and C (3.2%) coefficients were smaller than the relative precisions of the protocol designed to measure these coefficients (<4% and <6%, respectively). The reproducibility of the kinetic performance of these columns packed with sub-3µm core-shell particles is strongly dictated and tied to the reproducibility of the structure of the packed bed, e.g. the eddy dispersion A term. Figure 7 shows the column-to-column reproducibility of the reduced A term of naphthalene for six 4.6mm x 100mm (left graph) and six 2.1mm x 100mm (right graph) columns packed with the same batch of 2.7 µm Poroshell120-C_{18} shell particles and for reduced velocities larger than 3. It should be remembered that for such velocities, the precision on the measurement of the A term was better than 5% (which is represented by the thickness of the data point in these

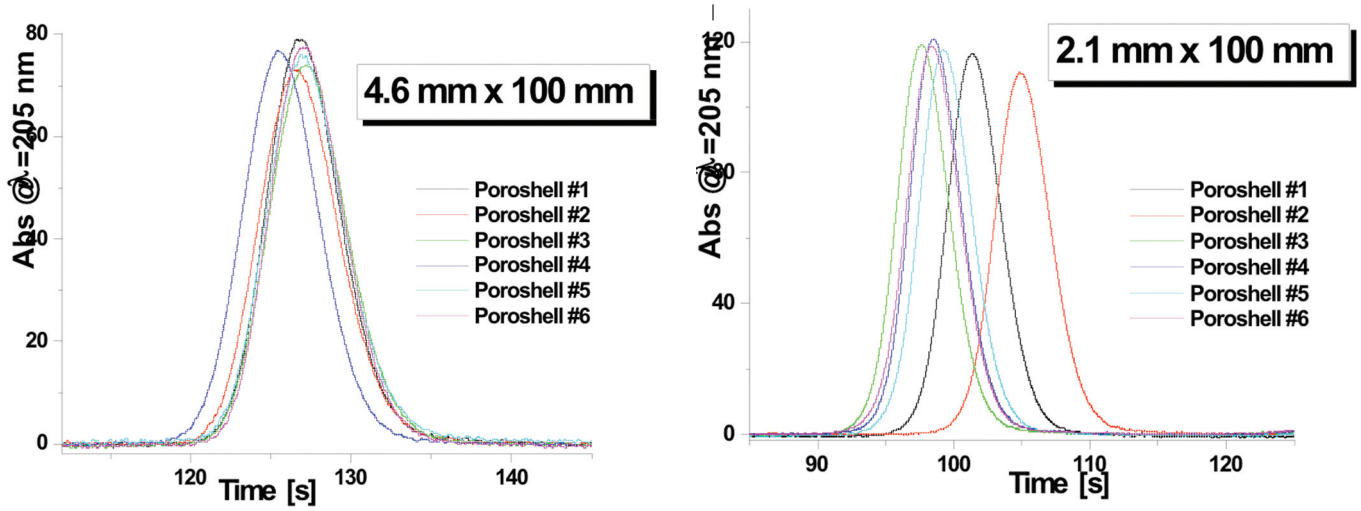

Figure 8: Column-to-column reproducibility of the elution profile of insulin for 4.6mm x 100mm (Left) and 2.1mm x 100mm (Right) columns packed with the same batch of 2.7µm Poroshell120-C_{18} core-shell particles. Same experimental conditions as in Figure 3. Sample volume injected: 1µL (4.6 mm I.D. columns) and 0.5µL (2.1mm I.D. columns).

graphs). Significant relative differences were observed between the 4.6mm I.D. columns #2 and #1 (+21%) and between the 2.1mm I.D. columns #6 and #4 (+13%). From a reduced velocity of 3 to 18, the average RSDs of the experimental eddy dispersion HETP terms were equal to 6.9% and 8.3% for the 4.6 and 2.1mm I.D. columns, respectively. Note that these RSD values obtained from the true moments of the peak profiles were about thrice larger than the RSDs measured from the USP convention.

For large biomolecules such as insulin and for the highest reduced velocities tested (ν> 100), the levels of column-to-column reproducibility for both the retention times and the column efficiencies were found similar to those measured for small molecules. Figure 8 shows the recorded peak profiles of insulin on the six 4.6mm I.D. (left graph) and on the six 2.1mm I.D. (right graph) Poroshell columns. For the wide columns, the RSDs of the elution times and column efficiencies are equal to 0.5 and 7.8%, respectively. For the narrow-bore columns, the RSD of the retention times increases to 4.5% whereas that of the column efficiency remains relatively low at 5.5%.

Conclusions

A meticulous investigation of mass transfer phenomena in 2.1 and 4.6 x 100mm I.D. columns packed with 2.7µm Poroshell120 EC-C_{18} core-shell particles provided a wealth of knowledge regarding the kinetic factors that control the efficiency of these columns for both small and large molecules. Unlike common propagated belief, the success of these shell particles in the separation of small molecules is not primarily due to the decrease of the solid-liquid mass transfer resistance Cν term (or the reduction of the average diffusion path). In fact, the contribution of this term to the total plate height was already negligible for columns packed with fully porous particles (<5%). The impact of axial diffusion is underestimated in RPLC for retained analytes at the optimum reduced velocities (ν~10). Indeed, the presence of the 1.7µm impermeable cores contributes to increase the optimum efficiency of columns packed with 2.7µm particles by more than 25 000 plates per meter, a significant gain. Most importantly, the exceptional performance of the 4.6mm I.D. columns packed with shell particles is caused by a reduction of the trans-column eddy dispersion term, which cannot be related to the tightness of the PSD of these particles. The true explanation for the enhanced homogeneity of the packed bed structure in the whole column is still unknown. This could be due to the surface roughness of the shell particles which would generate a high shear stress between the particles and between the wall and the particles, and therefore, a reduced strain during the bed consolidation. Remarkably, the trans-column eddy dispersion increases with decreasing the column diameter from 4.6mm to 2.1mm (intrinsic efficiency loss of 25%). The column-to-column reproducibility of the efficiency of these columns is similar to that previously reported 10 years ago for columns packed with conventional 5µm fully porous particles (RSDs of 2-3% from the USP convention and 7-8% from the numerical integration of the peak profiles).

Regarding the separation of large molecules, the Cν term governs the mass transfer mechanism as was originally expected when the first pellicular particles were prepared 50 years ago. The benefit of core-shell particles for the analysis of large molecules can be optimised by preparing new materials with a core-to-particle ratio around 0.9 and a porous shell with an average mesopore size as wide as 200 to 300 Å.

References

1. Cs. Horvath, B. Preiss, S. Lipsky, Anal. Chem. 39 (1967) 1422.

2. J.H. Knox, Anal. Chem. 38 (1966) 253.

3. J.R. Parrish, Nature 207 (1965) 402.

4. Cs. Horvath, S. Lipsky, Anal. Chem. 41 (1969) 1227.

5. Cs. Horvath, S. Lipsky, J. Chromatogr. Sci. 7 (1969) 109.

6. J. van Deemter, F. Zuiderweg, A. Klinkerberg, Chem. Eng. Sci. 5 (1956) 271.

7. U.D. Neue, HPLC Columns - Theory, Technology, and Practice. Wiley-VCH, Inc., New York, 1997.

8. J. Kirkland, Anal. Chem. 41 (1969) 218.

9. J. Kirkland, Anal. Chem. 43 (1971) 36A.

10. J. Kirkland, Anal. Chem. 64 (1992) 1239.

11. J. Kirkland, T. Langlois, J. De Stefano, Am. Lab. 39 (2007) 18.

12. J. Mazzeo, U. Neue, M. Kele, R. Plumb, Anal. Chem. 77 (2005) 460A.

13. F. Gritti, A. Cavazzini, N. Marchetti, G. Guiochon, J. Chromatogr. A 1157 (2007) 289.

14. F. Gritti, C. Sanchez, T. Farkas, G. Guiochon, J. Chromatogr. A 1217 (2010) 3000.

15. G. Guiochon, F. Gritti, J. Chromatogr. A 1218 (2011) 1915.

16. F. Gritti, I. Leonardis, J. Abia, G. Guiochon, J. Chromatogr. A 1217 (2010) 3819.

17. K. Horvath, F. Gritti, J.N. Fairchild, G. Guiochon, J. Chromatogr. A 1217 (2010) 6373.

18. A. Daneyko, S. Khirevich, A. Holtzel, A. Seidel-Morgenstern, U. Tallarek, J. Chromatogr. A 1218, (2011) 8231.

19. J.C. Giddings, Dynamics of Chromatography. Marcel Dekker, New York, 1965.

20. K. Kaczmarski, G. Guiochon, Anal.Chem. 79 (2007) 4648.

21. F. Gritti, G. Guiochon, J. Chromatogr. A 1218 (2011) 3476.

22. F. Gritti, G. Guiochon, J. Chromatogr. A 1221 (2012) 2.

23. F. Gritti, G. Guiochon, Chem. Eng. Sci. 66 (2011) 6168.

24. F. Gritti, G. Guiochon, J. Chromatogr. A 1218 (2011) 5216.

25. F. Gritti, G. Guiochon, AIChE 57 (2011) 333.

26. F. Gritti, G. Guiochon, Anal. Chem. 81 (2009) 2723.

27. F. Gritti, G. Guiochon, J. Chromatogr. A 1218 (2011) 4452.

28. P. Stevenson, F. Gritti, G. Guiochon, J. Chromatogr. A 1218 (2011) 8255.

29. H. Gao, P. Stevenson, F. Gritti, G. Guiochon, J. Chromatogr. A 1222 (2012) 81.

30. J.H. Knox, L. McLaren, Anal.Chem. 36 (1964) 1477.

31. D. Ludlum, R. Warner, H. Smith, J. Phys. Chem. 66 (1962) 1540.

32. P. Dunlop, C. Pepela, B. Steel, J. Am. Chem. Soc. 92 (1970) 6743.

33. F. Gritti, G. Guiochon, J. Chromatogr. A in preparation.

34. I. Halasz, M. Naefe, Anal. Chem. 44 (1972) 76.

35. J. Done, J. Knox, J. Chromatogr. Sci. 10 (1972) 606.

36. R. Endele, I. Halasz, K. Unger, J. Chromatogr. 99 (1974) 377.

37. C. Dewaele, M. Verzele, J. Chromatogr. 260 (1983) 13.

38. F. Gritti, T. Farkas, J. Heng, G. Guiochon, J. Chromatogr. A 1218 (2011) 8209.

39. A. Daneyko, A. Holtzel, S. Khirevich, U. Tallarek, Anal. Chem. 83 (2011) 3903.

40. S. Khirevich, A. Daneyko, A. Holtzel, A. Seidel-Morgenstern, U. Tallarek, J. Chromatogr. A 1217 (2010) 4713.

41. D.J. Gunn, Trans. Instn Chem. Engrs 47 (1969) T351.

42. F. Gritti, G. Guiochon, J. Chromatogr. A submitted for publication.

43. J.J. Kirkland, J.J. DeStefano, J. Chromatogr. A 1126 (2006) 50.

44. M. Kele, G. Guiochon, J. Chromatogr. A 830 (1999) 55.

45. M. Kele, G. Guiochon, J. Chromatogr. A 855 (1999) 423.

46. M. Kele, G. Guiochon, J. Chromatogr. A 869 (2000) 181.

47. M. Kele, G. Guiochon, J. Chromatogr. A 913 (2001) 89.

48. M. Kele, G. Guiochon, J. Chromatogr. A 830 (1999) 41.

49. J.J DeStephano, T.J. Langlois, J.J. Kirkland, J. Chromatogr. Sci.46 (2008) 254.